Journal of Hazardous Materials 215–216 (2012) 208–216

Contents lists available at SciVerse ScienceDirect

Journal of Hazardous Materials

journal homepage: www.elsevier.com/locate/jhazmat

Surface modified magnetic Fe_3O_4 nanoparticles as a selective sorbent for solid phase extraction of uranyl ions from water samples

Susan Sadeghi[a,*], Hoda Azhdari[a], Hadi Arabi[b], Ali Zeraatkar Moghaddam[a]

[a] Department of Chemistry, Faculty of Science, University of Birjand, P.O. Box. 97175/615, Birjand, Iran
[b] Magnetism and Superconducting Research Lab, Department of Physics, Faculty of Science, University of Birjand, P.O. Box. 97175/615, Birjand, Iran

ARTICLE INFO

Article history:
Received 27 June 2011
Received in revised form 20 February 2012
Accepted 21 February 2012
Available online 3 March 2012

Keywords:
Magnetic nanoparticle
Quercetin
Solid phase extraction
Response surface methodology
Uranyl ion

ABSTRACT

In this study, silica-coated magnetic nanoparticles modified with quercetin were synthesized by a sol–gel method. These magnetic nanoparticles were assessed as a new solid phase sorbent for extraction of uranyl ions from aqueous solutions. The crystal and chemical structures and magnetic property of the new sorbent were characterized by X-ray diffraction (XRD), transmission electron microscopy (TEM), Fourier transform infrared spectrophotometer (FT-IR), and vibration sample magnetometer (VSM). The experimental parameters affecting the extraction efficiency of uranyl ions from aqueous solutions using the synthesized sorbent were optimized by means of the response surface methodology. The adsorption equilibrium of uranyl ions onto the sorbent was explained by Langmuir isotherm and maximum monolayer adsorption capacity was found 12.33 mg/g. The synthesized sorbent was applied to extraction of uranyl ions from different water samples.

1. Introduction

Uranium is a radioactive metallic element which is chemically active at its pure form. However, uranium and its compounds are highly toxic and lead to kidney failure or even death. The World Health Organization (WHO) establishes that the maximum uranium concentration in drinking waters should be less than 15 $\mu g\,L^{-1}$, while this value in spring waters is recommended to be less than 20 $\mu g\,L^{-1}$ [1,2]. But depending on location, the level of uranium in waters is varied. It is difficult to determine directly the extremely low concentration of uranium in the presence of relatively high concentration of other diverse ions. Therefore, a refined analytical method must be employed to detect such low concentrations [3]. Preconcentration/extraction method is an approach that can be used to improve the analytical detection limit and sensitivity of the method. Solid phase extraction (SPE) is one of the most effective preconcentration methods because of its simplicity, ability to achieve higher enrichment factor and accessibility to selective sorbents [4]. So far, several selective solid phase sorbents for preconcentration of uranyl ions from aqueous solutions have been prepared either by physical loading or chemical binding of selected chelating reagents onto different supports [5–17]. Nevertheless, search for new sorbents with high surface area, low swelling behavior and stable at a wide pH range have been the major objective of many researches.

Nano materials are new solid materials that have attracted to SPE methods substantially due to their special properties [18]. Recently, magnetic nanoparticles as adsorption materials have been employed for removal of trace metal analytes from water samples [19–21]. Magnetic nanoparticles are particularly attractive due to their unique properties such as excellent magnetic responsivity, high dispersibility, relatively large surface area and easiness of surface modification which enable them to have a wide range of potential applications in biological, environmental and food analysis [22,23]. But, these nanometer size materials are not selective to extraction of metal ions especially in complicated matrices. It has been proven that the formation of an inert coating materials such as silica on the surface of magnetic nanoparticles not only can prevent aggregation of these particles in liquids and improves their chemical stability, but also due to the presence of numerous hydroxyl groups on the surface of silica, it can readily link to organic functional groups of metal chelates [24]. This modification of the surface of magnetic nanoparticles plays an important role in the selective preconcentration and separation of analytes [19].

Quercetin may be considered as one of the most biologically active and common dietary flavonols. It has the ability to form complexes with some metal ions and may sequester these metal ions and prevent them from irretrievable damages on human health and environment [25–27]. To our knowledge, quercetin has not previously been immobilized on the

* Corresponding author. Fax: +98 561 2502009.
E-mail address: ssadeghi@birjand.ac.ir (S. Sadeghi).

0304-3894/$ – see front matter © 2012 Elsevier B.V. All rights reserved.
doi:10.1016/j.jhazmat.2012.02.054

surface of magnetic nanoparticles. So we used quercetin to modify surface of silica coated Fe_3O_4 magnetic nanoparticles and explored the metal sorption behavior of the new resulted chelating sorbent in batch extraction mode. Collecting the sorbent from aqueous solution was performed easily using a permanent magnet.

The preliminary experiments showed the good tendency of the sorbent to uranyl ions, so in the next step, the predominant experimental factors affecting the extraction efficiency of uranyl ions onto the new sorbent were optimized. Although traditional methods of optimization with successive variations in factors such as a one factor at a time approach are still used and well accepted in optimization, but it requires a relatively large number of experiments to be conducted which is time consuming and possible interactions between factors cannot be considered [28]. Statistical experimental designs, on the other hand, based on the response surface methodology (RSM) are alternative methods to study the effects of various parameters simultaneously affecting extraction efficiency [29]. The objective of the present study is to investigate the feasibility of using the new synthesized sorbent for extraction of uranyl ions from aqueous solution, and to optimize the factors to impact maximum extraction efficiency using central composite design (CCD) based on RSM. The most important factors used are sample pH, the amount of weight of sorbent to sample volume ratio (mg/mL) and contact time (min).

2. Materials and methods

2.1. Materials

All used chemicals had analytical grade and were provided from Merck (Darmstadt, Germany). Stock solution of uranyl ions was prepared by dissolving an appropriate amount of uranium nitrate in deionized water and diluted with the buffer. Buffer solutions were prepared from 0.01 mmol mL^{-1} sodium acetate–acetic acid. The stock solutions of the metal ions (1000 mg/L) were prepared by dissolving metal nitrates in deionized water. The 0.1% Arsenazo III solution was prepared by dissolving 0.1 g of the reagent in 100 mL of deionized water.

2.2. Apparatus

Ultrapure water was generated using AquaMax water purification system (Younglin, Anyang, Korea). The magnetite nanoparticles were characterized by transmission electron microscopy (TEM), Fourier transform infrared spectroscopy (FT-IR), X-ray powder diffraction (XRD) and vibration sample magnetometer (VSM). TEM micrographs were obtained by a LEO system (model 912 AB) operating at 120 kV. The FTIR spectra (400–4000 cm^{-1}) were recorded using KBr pellets by VERTEX 70 FT-IR spectrophotometer (Bruker, Germany). XRD patterns of NPs were collected using Cu Kα radiation on a D8 Advanced Bruker X-ray diffractometer (Bruker, Germany) at room temperature with a step size of 0.04° (2θ/s). Magnetic properties of NPs were investigated by a Lake-shore VSM model 7400.

2.3. Preparation of the sorbent

2.3.1. Synthesis of modified magnetic nanoparticles

The Fe_3O_4 nanoparticles were synthesized via a chemical co-precipitation method with $FeCl_2$ and $FeCl_3$ according to Ref. [30]. The Silica coated magnetic nanoparticles with a dense silica shell on the surface of Fe_3O_4 nanoparticles were prepared by the Stöber method through the sol–gel reaction of tetraethyl orthosilicate (TEOS) [31]. Subsequently, the amino silicate shell was formed onto the dense silica shell using 3-aminopropyl triethoxysiliane (APS) in dry toluene. For this purpose, silica coated Fe_3O_4 nanoparticles were dispersed into dry toluene (15 mL) and 1 mL of APS in 5 mL toluene was added to the solution with stirring for 12 h. The resulting material was washed four times with dry toluene and ethanol, respectively, and finally dried under vacuum.

2.3.2. Immobilization of quercetin onto modified magnetic nanoparticles

To prepare the sorbent, 1 mmol of quercetin in 20 mL of dried ethanol was added to a suspension of aminosilica coated Fe_3O_4 nanoparticles and was refluxed for 24 h. The resulting material (abbreviated QASM) was washed with ethanol until the excess quercetin removed. Then, it was dried under vacuum. The schematic presentation of the synthesized material is shown in Fig. 1.

2.4. General procedure

100 mg of QASM as sorbent were put into a 250 mL polyethylene bottle. Then, 100 mL of the buffered uranyl ion solution was added into the bottle. Under continuous mechanical stirring of the mixture for 30 min, the extraction of uranyl ions from aqueous solution onto the sorbent was allowed to proceed at room temperature. After standing for 1 min, the QASM adsorbed uranyl ions were completely gathered to one side of the solution under a strong external magnetic field and the clear supernatant was directly decanted. The initial concentration (C_i) and equilibrium concentration of uranyl ions in the supernatant (C_e) were determined by spectrophotometric method using Aresenazo III as chromogenic indicator [16]. The amount of uranyl ions adsorbed on the sorbent was evaluated by the extraction efficiency (E%) according to Eq. (1):

$$E(\%) = \frac{C_i - C_e}{C_i} \times 100 \quad (1)$$

2.5. Sample preparation

Two kinds of water samples were utilized in this study: mineral water (Nesteleh Mineral water Co.) and underground water. The samples were collected from Ghaleh Doghtar spring (northwest of Tehran, Iran) and Shokat Abad Ghanat (north of Birjand, Iran), respectively. The water samples were stored in polyethylene container in refrigerator for further usage after they were acidified with concentrated HNO_3. Before the analysis, the water samples were also filtered through a 0.45 μm membrane filter.

2.6. Statistical design and data analysis

In response surface methodology (RSM), a number of experiments are performed in which changes are made in the input variables in order to identify the reasons for changes in the output response. The most important variables are selected based on the preliminary tests undertaken to assess the tendencies of the factors and which have the greatest influence on the response. In the present study, based on preliminary experiments, three main factors that affect the extraction efficiency of uranyl ions onto the sorbent (response) are sample pH (A; 3–4), contact time (B; 15–45 min) and the sorbent weight to sample volume ratio (C; 0.3–1.0 mg/mL). Two other factors, i.e. temperature and stirring rate were kept constant during the extraction at 25 °C and 300 rpm, respectively. The central composite design (CCD) as a popular second order polynomial design is most widely used to approach of RSM [32] and was used to build a predictive model of the extraction efficiency response. In CCD, three factors were considered in the two level factorial design (2^K design; k = number of main factors).

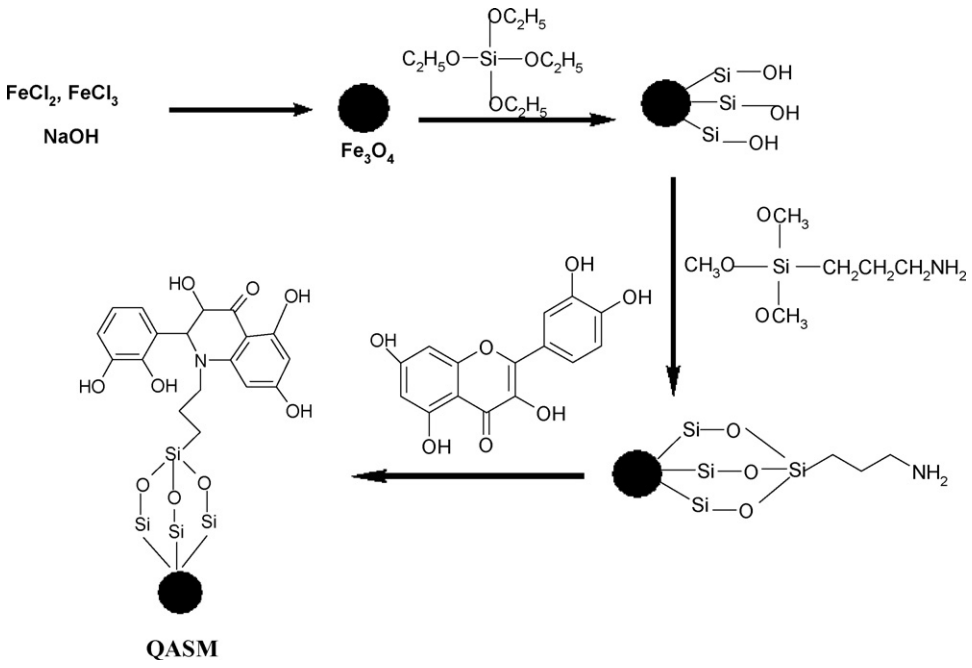

Fig. 1. Scheme illustration of the preparation of QASM.

Two values, a minimum and a maximum, coded with −1 and +1, were tested for each factor. Moreover, the CCD combines this factorial design with some additional points (star points or axial point; 2 K) and at least one point at the center that allow estimation of curvature [37]. If the distance from the center of the design space to factorial point is ±1 unit for each factor, the coded distance from the center of the design space to star points is $\pm\alpha$ with $|\alpha| > 1$ (coded α was 1.67 in this study). The corresponding factors and their levels are summarized in Table 1. Only two-way interactions were considered and quadratic model was fitted to the experimental data. To examine the combined effects of the three independent factors on the response, the experimental design comprising 20 experiments (8 experiments of factorial design for three factors, 6 experiments for the star points and 6 experiments for centre points) was performed. The experiments were run in a random manner in order to minimize the effect of uncontrolled variables [38]. The run time was not short enough to perform all 20 experiments during one working day, so they were divided into three blocks. On the other hand, we blocked the experiments to remove the expected variation caused by some changes during the course of the experiment.

Analysis of variance (ANOVA) was performed to characterize the coefficients of the quadratic equation. The quality of the fit of quadratic model was determined from the correlation coefficient value. The significance and adequacy of the model was assessed from the *F*-value (Fisher variation ratio), probability value (Prob > *F*), and the value of adequate precision. The data analysis was performed using Design-Expert Version 6.0.6 statistical software (Stat-Ease Inc., Minneapolis, MN, USA). Regression analysis was used to fit the equation developed and evaluate the statistical significance of the equation.

Table 1
Factors, their symbols and levels for central composite design.

Factors	Symbol	Levels				
		$-\alpha$	−1	0	+1	$+\alpha$
pH	A	2.7	3	3.5	4	4.3
Contact time (min)	B	6	15	30	45	54
Weight (mg)/volume (mL)	C	0.08	0.3	0.65	1.0	1.22

3. Results and discussion

The magnetic nanoparticles could be directly coated with amorphous silica via the hydrolysis of a sol–gel precursor TEOS. The iron oxide surface has a strong affinity toward silica, so no primer is required to promote its deposition and adhesion to silica. A surface active agent of APS was employed as a binder to immobilize quercetin onto the silica coated Fe_3O_4 nanoparticles producing a selective magnetic sorbent for extraction of uranyl ions from aqueous solutions.

To determine the suitability of the prepared magnetic sorbent in extraction of uranyl ions, the extraction efficiency of the sorbent for Th^{4+}, La^{3+} and Ce^{3+} ions was evaluated. These ions were chosen due to similar chemical behaviors with respect to uranyl ions. Furthermore, extraction of some transition metal ions using the prepared sorbent was investigated. Herein, aliquots of 100 mL of solutions containing 10 μmol mL^{-1} of metal ions were equilibrated with 100 mg of the QASM for 1 h. The extraction efficiency of the sorbent for the respective metal ions was calculated. The results are illustrated in Fig. 2. As can be seen, the sorbent showed high affinity to extract uranyl ions. Then, using the new developed sorbent; the optimization process was performed on extraction of uranyl ions from aqueous solution in batch extraction mode.

3.1. Characterization of modified NPs

In order to fully characterize the inorganic core and the organic shell of the synthesized magnetic nanoparticles for morphology, structure and magnetic properties, different techniques such as TEM, XRD, IR and VSM were used. Fig. 3 shows the typical TEM images of the magnetic nanoparticles, silica coated magnetic nanoparticles and QASM. Most of the produced Fe_3O_4 nanoparticles have sizes less than 15 nm which are shown in Fig. 3a. The condensation of silica on the surfaces of the magnetic cores resulted in a fairly core–shell like structure (shown in Fig. 3b) with dark colored magnetic nanoparticles core and a light colored shell having an average thickness of about 3 nm. Fig. 3c illustrates that the size of QASM is ca. 20–25 nm.

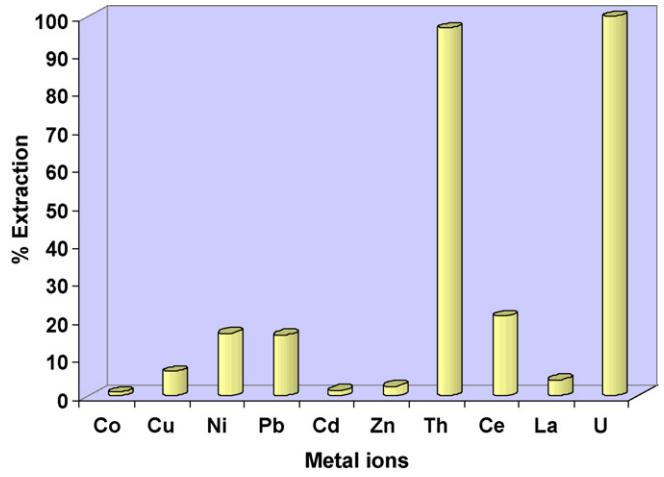

Fig. 2. Extraction efficiencies of some metal ions using 100 mg of the sorbent (conditions: 100 mL solution of 10 μmol mL^{-1} of cations at pH 4.0, contact time: 1 h).

To affirm the structure of magnetic nanoparticles and silica coated magnetic nanoparticles, X-ray diffraction patterns (XRD) were employed. As shown in Fig. 4, the powder XRD pattern of the synthesized magnetic nanoparticles was close to the pattern for crystalline magnetite Fe_3O_4 [33]. Using the most intense peak in Fe_3O_4 nanoparticles XRD pattern, the particle sizes of approximately 10–17 nm was estimated by the Debye–Scherer formula [34], which was consistent with the results obtained from the TEM image. The characteristic peaks of pure Fe_3O_4 nanoparticles at $2\theta = 30.1^\circ, 35.4^\circ, 43.9^\circ, 53.4^\circ, 57.0^\circ$ and 62.6° were also observed for silica coated Fe_3O_4 nanoparticles confirming the presence of the crystalline structure of the magnetite. Here, the intensity of the peaks decreases and become slightly wide indicating the occurrence of coating of non-magnetic and amorphous silica shell onto the surface of Fe_3O_4.

Fe_3O_4 nanoparticles, silica coated Fe_3O_4 nanoparticles and QASM were identified using Fourier transform infrared (FTIR) spectrometry. The resulting spectra are shown in Fig. 5. The spectrum of Fe_3O_4 nanoparticles (Fig. 5a) showed a strong absorption band at 576 nm which was assigned to the Fe–O vibration frequency of magnetite. The observed features around 1102 cm^{-1} for silica-coated magnetic nanoparticles (Fig. 5b) indicated to Si–O–Si and Si–O–H stretching vibrations. The presence of additional peaks centered at 808 cm^{-1} resulted from Si–O vibration [35]. The spectrum of the synthesized QASM (Fig. 5c) showed absorption bands at 1628 and 1078 cm^{-1} (broad), which were assigned to the stretching vibrations of (OH) and (OH)/SiO_2 overtone, respectively. The appearance of new bands at 1420, 1473 and 1512 cm^{-1} referred to vibration frequencies of (C–OH) and (C–N–C) bonds while the presence of absorption bands around 2865 cm^{-1} and 2940 cm^{-1} corresponded to symmetrical and asymmetrical of CH_2 stretching vibrations. A broad absorption band was found around 3299 cm^{-1} that attributed to stretching vibration of hydroxyl groups in the quercetin molecule. Consequently, these FT-IR spectra provided supportive evidence that quercetin attached to Fe_3O_4 nanoparticles via the displacement of pyran oxygen with nitrogen of propylamine.

The magnetic properties of the synthesized nanoparticles were also studied by a VSM. Fig. 6 shows the hysteresis loops of the Fe_3O_4, silica coated Fe_3O_4 and QASM at room temperature. The saturation magnetization, M_s, of bulk magnetite (92 emu g^{-1})[36] was reduced to 57 emu g^{-1} for magnetite nanoparticles. It is known that the magnetization of a magnetic particle in an external field is proportional to its size value. Therefore, a smaller saturation magnetization value for the magnetite nanoparticles compared to the

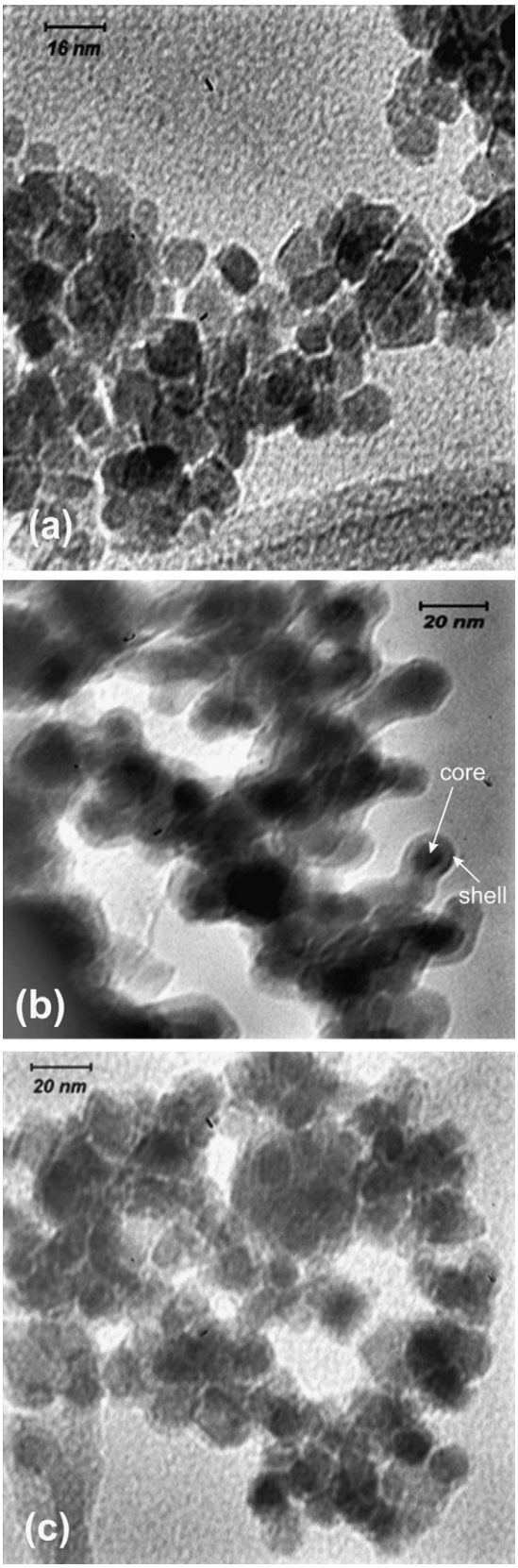

Fig. 3. TEM images of (a) Fe_3O_4 nanoparticles (b) silica coated Fe_3O_4 nanoparticles and (c) QASM.

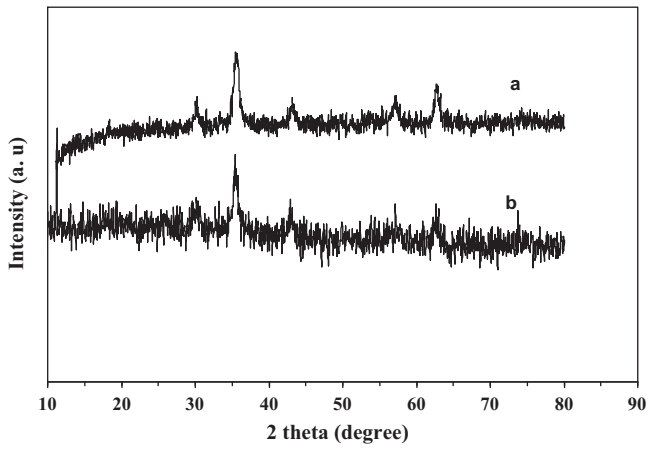

Fig. 4. XRD patterns of (a) Fe_3O_4 nanoparticles and (b) silica coated magnetite nanoparticles.

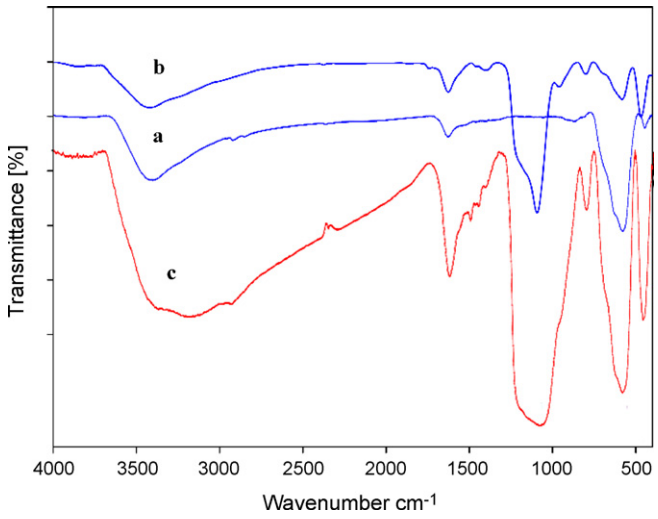

Fig. 5. FTIR spectra of (a) Fe_3O_4 nanoparticles, (b) silica coated Fe_3O_4 nanoparticles and (c) QASM.

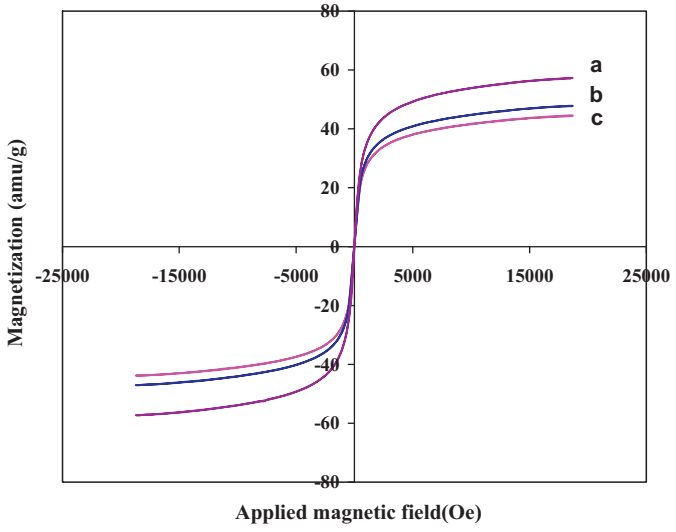

Fig. 6. VSM magnetization curves of (a) Fe_3O_4 nanoparticles (b) silica coated Fe_3O_4 nanoparticles and (c) QASM measured at 300 K.

bulk material is reasonable. The saturation magnetic moments of the silica coated Fe_3O_4 nanoparticles and quercetin immobilized Fe_3O_4 nanoparticles reached to 47 emu g^{-1} and 44 emu g^{-1}, respectively. In spite of these low magnetization values with respect to magnetization of pure Fe_3O_4 nanoparticles, which was owing to decrease in the surface moments of the magnetic nanoparticles by non-magnetic silica coating, but it is still sufficient for magnetic separation by a conventional magnet.

3.2. Optimization of sorption

A quadratic model correlating extraction efficiency and interactive variables based on CCD design model is evolved by Design Expert software. This model is consisted of three principle effects for three input factors, three two–factor interaction effects and three curvature effects. The relationship between the extraction efficiency of uranyl ions onto the sorbent and input factors is given in final coded equation as below:

$$E(\%) = +84.79 + 23.52A + 2.91B + 22.21C - 10.24A^2 - 1.59 \times B^2 - 10.38C^2 - 2.25AB - 8.10AC - 3.38BC \quad (2)$$

The magnitude of the coefficients in Eq. (2) indicates to the intensity of the influence, while the sign denotes the nature of influence of factors.

To evaluate the model and the significance of these effects, the analysis of variance (ANOVA) was conducted. The results of ANOVA for quadratic model for the three variables through F and P values are summarized in Table 2. The F value in this Table is the ratio of mean square error due to the regression to the mean square of the pure error (experimental error). The high value of F indicates that most of the variation in the response can be explained by the regression equation. The associated P value is used to estimate whether F is large enough to indicate statistical significance.

In this model, A and C had a highly significant effect ($P < 0.0001$) at the maximum response. Moreover, the quadratic terms A^2, C^2, and AC had also a significant effect ($P < 0.05$). Values greater than 0.05 indicate the model terms are not significant [39].

The values of Prob > F (P values) less than 0.050 indicate the statistical significance of the model. According to the Table 2, the model F value for response is 40.60 proving the significance of the model. The lack-of-fit P value was found to be 0.3332 showing that the lack of fit is not important with respect to the pure error.

To evaluate how the model satisfies the assumptions of ANOVA, a normal probability plot of the residuals provided by the Design Expert software and the result is illustrated in Fig. 7. The points on this plot lie reasonably close to a straight line confirming that the residuals follow a normal distribution with mean of zero, concluding again that A, C, A^2, C^2 and AC are the significant factors. Also, the plots of residuals versus different variables such as predicted values, run order, and factors were also depicted (not shown here) giving a minimum residual for the prediction of each response reaffirmed our findings.

The goodness of fit of the proposed second polynomial model is characterized by the coefficient of determination (R^2) and adjusted R^2. R^2 is a measure of the variation of the experimental points around the regression line, while the adjusted R^2 is used to adjust the number of experimental terms in the model to improve correlation between the variables and the response. R^2 and adjusted R^2 for the selected model were found to be 0.9786 and 0.9545, respectively. The lower value of the adjusted R^2 in comparison with R^2 value indicates the goodness of data fit.

For the graphically interpretation of the interactions, the three dimensional response surface plot (3D) of the model is used to show the relationship between the response and the level of each factor. By considering the significant terms in the model, the response of

Table 2
Analysis of variance (ANOVA) for response surface quadratic model for uranyl extraction by quercetin immobilized Fe_3O_4 nanoparticles (QASM).

Source	Sum of squares	dF[a]	Mean square	F-value[b]	P-value[c] Prob > F	
Block	192.40	2	96.20	2.06	0.3817	Not significant
Model	17159.28	9	1906.59	40.60	<0.0001	Significant[e]
A	7256.80	1	7256.80	154.33	<0.0001	
B	111.22	1	111.223	2.37	0.1626	
C	6565.50	1	6565.50	139.63	<0.0001	
A^2	1303.51	1	1303.51	27.72	0.0008	
B^2	31.45	1	31.45	0.67	0.4371	
C^2	1415.57	1	1415.57	30.11	0.0006	
AB	40.50	1	40.50	0.86	0.3805	
AC	524.88	1	524.88	11.16	0.0101	
BC	91.13	1	91.13	1.94	0.2014	
Residual	376.17	8	47.02			
Lack of fit	282.15	5	56.43	1.80	0.3332	Not significant
Pure error	94.02	3	31.34			
Cor. total[d]	17727.85	19				

[a] Degrees of freedom.
[b] Test for comparing model variance with residual (error) variance.
[c] Probability of finding the observed *F*-value if the null hypothesis is true.
[d] Totals of all information corrected for the mean.
[e] Significant at $P < 0.05$

the model is depicted versus the two experimental factors while the third one is constant at its central level. Fig. 8 shows the 3D plot of the response versus sample pH and the ratio of weight of the sorbent to the sample volume at constant contact time of 30 min. As shown in the Fig. 8, increase in both sample pH and sorbent weight to sample volume ratio increase in the extraction efficiency of uranyl ions from aqueous solution till the equilibrium is approached. Maximum response occurred at pH > 3.7. The pH of the sample solution had a pronounced influence on the response. The pH effect was studied in the range of 3.0–4.0 because the hydroxyl groups of quercetin can be protonated at low pH. At higher pH values than 4, the uranyl ions might hydrolyze to form species such as UO_2OH^+ and $(UO_2)_2(OH)_2$, and the response decreases. Adsorption with high sorbent weight to the sample volume ratio favored maximal extraction efficiency of uranyl ions due to the greater availability of the sorbent surface at high amount of sorbent. The optimal extraction conditions were pH, 3.70; ratio of the sorbent weight to sample volume, 0.77 and contact time, 30 min. The maximum observed on the response surface would thus correspond to a mean extraction efficiency response of 94.5%.

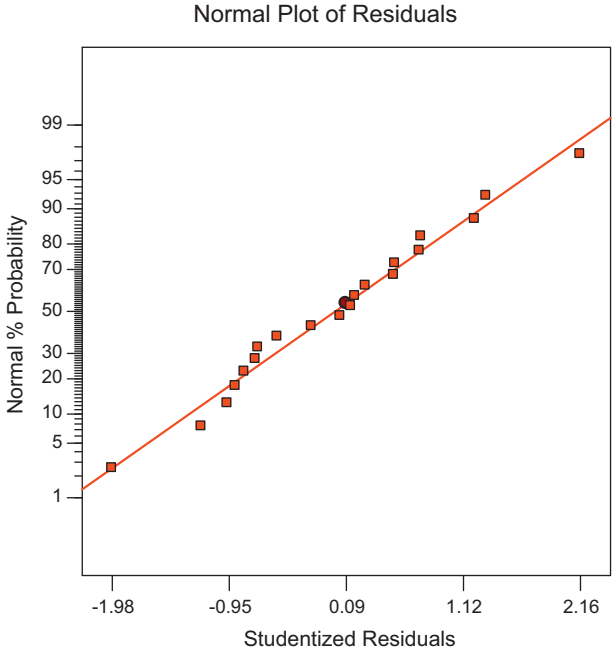

Fig. 7. Normal plot of probability (%) versus studentized residuals.

3.2.1. Adsorption capability

To determine the adsorption capacity, 100 mL solutions of various concentrations of uranyl ions at pH 3.7 were equilibrated with 77 mg of QASM. The equilibrium binding amount of quercetin immobilized magnetic nanoparticles towards uranyl ions were calculated according to the following equation:

$$q_e = (C_i - C_e)Vm^{-1} \quad (3)$$

where q_e is the adsorption capacity (mg/g) based on the dry weight of QASM, C_i and C_e are the initial and equilibrium concentrations (mg/L) of uranyl ions in solution, m is the weight of the sorbent in g and V is the volume of the aqueous solution in L. The plot of q_e versus C_e showed a typical Langmuir isotherm (Fig. 9). An adsorption isotherm describes the correlation between adsorbate extraction by the sorbent and the adsorbate concentration remaining in the solution in certain model. This isotherm [40] describes monolayer adsorption and is based on the assumption that all the adsorption sites have equal adsorbate affinity and that adsorption at one site does not affect adsorption at an adjacent site, representing by the following Eq. (4):

$$q_e = \frac{q_{max}K_LC_e}{1 + K_LC_e} \quad (4)$$

where q_{max} is the maximum adsorption capacity (mg/g) and K_L is the Langmuir equilibrium constant (L/mg). The values of q_{max} and K_L were calculated from the slope and intercept of the linear form of the Langmuir isotherm which were found to be 12.33 mg/g and 0.088 L/mg, respectively. The theoretical q_{max} value calculated from the Langmuir adsorption model was close to the experimental value (10.0 mg/g). As shown in the inset in Fig. 9, the plot of C_e/q vs. C_e yielded a straight line ($R^2 = 0.9905$) revealing that the adsorption of uranyl ions obeys the Langmuir isotherm. In addition, the capacity of Fe_3O_4 and silica coated Fe_3O_4 nanoparticles as sorbents for extraction of uranyl ions under the optimized conditions were evaluated and found 2.73 and 4.33 mg/g, respectively. These finding indicate that the modification of magnetic nanoparticles with quercetin greatly increases the adsorption capacity of Fe_3O_4 nanoparticles.

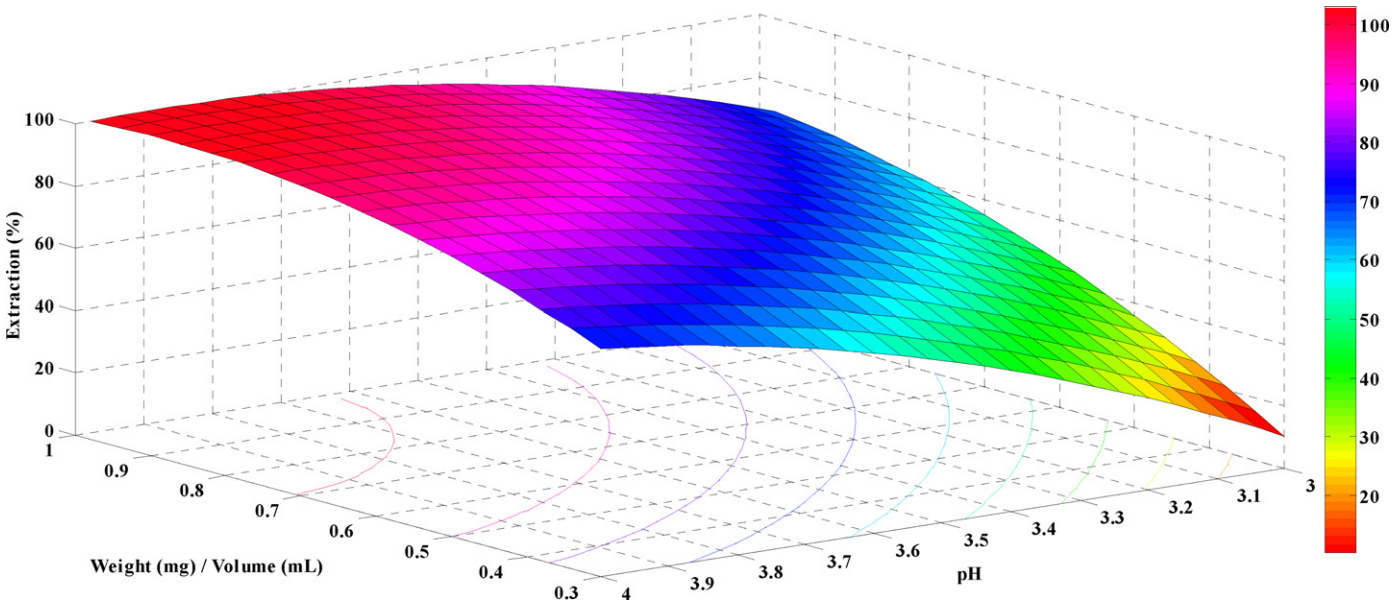

Fig. 8. Response surface 3D graph for extraction of uranyl ions by QASM as sorbent versus pH and the sorbent weight to sample volume ratio at 30 min.

Table 3
Effect of coexisting ions on extraction of 2.7 μg mL^{-1} uranyl ions from aqueous solution under optimum condition.

Ion	Tolerance limit (μg mL^{-1})
K^+, Na^+	250
Ca^{2+}, Mg^{2+}	250
Zn^{2+}	200
Pb^{2+}	310
Co^{2+}, Ni^{2+}	120
Cd^{2+}	225
La^{3+}, Ce^{3+}, Th^{4+}	14

3.3. Interference effect

The optimal experimental conditions described above were used to study the interference effect of diverse ions during the extraction of uranyl ions. The tolerance limit was set as the amount of ions that reduce the extraction efficiency of uranyl ions to less than 95% and compete for adsorption on the sorbent. The obtained tolerance limits are summarized in Table 3. The results imply that the developed sorbent is selective to uranyl ions with regard to commonly found interferences.

3.4. Analytical performance

Under the optimal experimental conditions, the developed sorbent offered good linearity (r = 0.9995) with a calibration function for the extraction of uranyl ions in the concentration range of 0.068–6.75 μg mL^{-1}. The detection limit of the method based on three times of standard deviation of the blank divided by the slope of the calibration curve was found to be 4.6 ng mL^{-1}. In order to study the precision of the developed method, six replicate extractions of solutions containing 2.7 μg mL^{-1} of uranyl ions were performed and the relative standard deviation (RSD%) was obtained 3.2%. The performance of the developed sorbent in comparison with other sorbents reported in the literatures [41–46] for extraction of uranyl ions is given in Table 4. Accordingly, the present sorbent showed high capacity and short extraction time which can be attributed to the large surface area and rapid dynamic extraction of the quercetin immobilized Fe_3O_4 nanoparticles. In addition, the methodology described here is simple in the viewpoint of collection

Table 4
Comparison of the present modified Fe_3O_4 nanoparticles sorbent (QASM) with the other sorbents for extraction of uranyl ions in water samples.

Sorbent	Technique	RSD (%)	Capacity (mg/g)	Equilibration time (h)	Ref.
Carboxy methylated polyethyleneimine modified nanoporous silica	Batch SPE/ICP-AES	NM	6.33–124	12	41
Amidoximated polyglycidyl methacrylate microbeads	On line SPE/DPP	NM	1.07	NM	42
Tetramethyl malonamide chelating resin beads	Batch SPE/CCD - ICP-OES	NM	135	1	43
Hematite	Batch SPE/Micro titration	<10	3.36–3.54	6 h	44
Silica modified with xylenol orange	Batch SPE/Fluorimetry	15	10	0.5	45
Unsaturated sugar derivative MOADDTCEXHEF	Batch SPE/Spectrophotometry with dibenzoyl methane-trioctyl phospine	<5	40.2	0.5	46
Quercetin modified Fe_3O_4 nanoparticles	Batch SPE/Spectrophotometry with Arsenazo III	3.2	12.3	<0.5	This work

NM, not mentioned; DDP, differential pulse polarography.

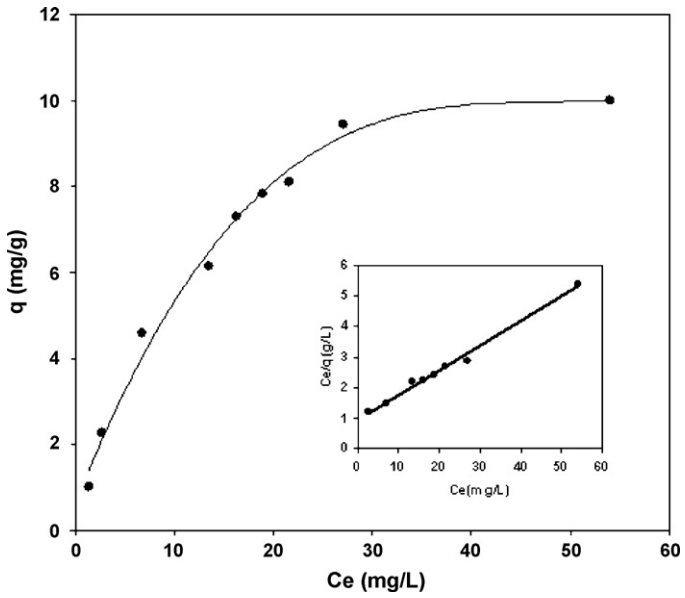

Fig. 9. Equilibrium isotherm for the extraction of uranyl ions on the QASM at pH 3.7 and 25 °C. The inset illustrates the linear dependence of C_e/q_e on C_e (77 mg sorbent; 100 mL sample).

Table 5
Recovery of the uranyl ions spiked in the two water samples by applying the developed sorbent.

Sample	Result
Ground water[a]	
Not spiked	–
Spiked (20 μg L^{-1})	20.2 ± 1.2
Recovery (%)	93.3 ± 2.9[c]
Mineral water[b]	
Not spiked	–
Spiked (20 μg L^{-1})	20.2 ± 1.2
Recovery (%)	85.7 ± 2.7[c]

[a] This water contains Ca^{2+} 143.9 μg mL^{-1}, Mg^{2+} 876.8 μg mL^{-1}, Na^{+} 1 μg mL^{-1}, K^{+} 15.4 μg mL^{-1}.
[b] This water contains Ca^{2+} 31.8 μg mL^{-1}, Mg^{2+} 6.5 μg mL^{-1}, Na^{+} 1 μg mL^{-1}, K^{+} 0.4 μg mL^{-1}, HCO_3^- 142.8 μg mL^{-1}, F^- 0.07 μg mL^{-1}, Cl^- 1.5 μg mL^{-1}, SO_4^{2-} 4 μg mL^{-1}, NO_3^- 3.5 μg mL^{-1}.
[c] Based on triplicate analysis.

of the sorbent from the solution and the sorbent is relatively inexpensive material compared with other adsorptive materials.

3.5. Analytical application

In order to validate the suitably of the developed sorbent in preconcentration of uranyl ions, it was applied to extraction of uranyl ions in ground water and mineral water samples containing varying amounts of diverse ions. The characteristics of water samples are presented in Table 5. No uranyl ions were found in the tested waters, so 250 mL of water samples spiked with 20 ng mL^{-1} uranyl ions and were treated by the SPE procedure as described in the experimental section. The concentration found for uranyl ions in water samples have been summarized in Table 5. In spite of the constituent in water samples which might compete for interaction with the sorbent, the uranyl ion recoveries were acceptable.

4. Conclusions

A new sorbent based on magnetite nanoparticles was synthesized and modified with quercetin. The potential application of the modified nanoparticles as a sorbent in the extraction of uranyl ion from environmental waters was investigated. The developed method has the advantage of the sample introduction and extraction of uranyl ions in one step. Furthermore, the magnetic property of the sorbent provides a rapid and easy separation of the sorbent from aqueous solution just by using a permanent magnet without filtration. The method is very suitable for rapid adsorption of uranyl ions from large volume of sample solution.

Acknowledgement

Authors are grateful to the Research Council of the Birjand University for funding this work.

Appendix A. Supplementary data

Supplementary data associated with this article can be found, in the online version, at doi:10.1016/j.jhazmat.2012.02.054.

References

[1] World Health Organization, Guidelines for Drinking Water Quality, vol. 2, 2nd ed., WHO, 1998.
[2] The Brazilian Environmental Council (Conama) National Council of Environment, Resolution number 357, Reference Base http://www.cetesb.sp.gov.br/Agua/praias/res-conama/357-05pdf.
[3] T. Prasada Rao, P. Metilda, J.M. Gladias, Preconcentration techniques for uranium(VI) and Thorium (IV) prior to analytical determination: an overview, Talanta 68 (2006) 1047–1064.
[4] J.S. Fritz, Analytical Solid Phase Extraction, 1st ed., New York, Wiley-VCH, 1999.
[5] M.A.A. Akl, I.M.M. Kenawy, R.R. Lasheen, Organically modified silica gel and flame atomic absorption spectrometry: employment for separation and preconcentration of nine trace heavy metals for their determination in natural aqueous systems, Microchim. Acta 78 (2004) 143–156.
[6] T.E. Milja, K.P. Prathish, T.P. Rao, Synthesis of surface imprinted nanospheres for selective removal of uranium from simulants of Sambhar salt lake and ground water, J. Hazard. Mater. 188 (2011) 384–390.
[7] Y. Zhao, C. Liu, M. Feng, Z. Chen, S. Li, G. Tian, L. Wang, J. Huang, S. Li, Solid phase extraction of uranium (VI) onto benzylthiourea anchored activated carbon, J. Hazard. Mater. 176 (2010) 119–124.
[8] G.E. Fryxell, W. Chouyyok, R.D. Rutledge, Design and synthesis of chelating diamide sorbents for the separation of lanthanides, Inorg. Chem. Commun. 14 (2011) 971–974.
[9] F.A. Aydin, M. Soylak, Solid phase extraction and preconcentration of uranium (VI) and thorium (IV) on Duolite XAD 761 prior to their inductively coupled plasma mass spectrometric determination, Talanta 72 (2007) 187–192.
[10] V.K. Jain, A. Handa, R. Pandya, P. Shirvastav, K.K. Agrawal, Polymer supported calix[4]-arene-semicarbazone derivative for separation and preconcentration of La(III), Ce(III), Th(IV) and U(VI), React. Funct. Polym. 51 (2002) 101–110.
[11] T. Prasada Rao, R. Kala, S. Daniel, Metal ion-imprinted polymers-novel materials for selective recognition of inorganics, Anal. Chim. Acta 578 (2006) 105–116.
[12] L. Zhao, J. Sun, Y. Zhao, L. Xu, M. Zhai, Removal of hazardous metal ions from wastewater by radiation synthesized silica-graft-dimethylaminoethyl methacrylate adsorbent, Chem. Eng. J. 170 (2011) 162–169.
[13] M. Merdivan, S. Seyhan, C. Gok, Use of benzoylthiourea immobilized on silica gel for separation and preconcentration of uranium(VI), Microchim. Acta 154 (2006) 109–114.
[14] S. Sadeghi, D. Mohammadzadeh, Solid phase extraction—spectrophotometric determination of uranium (VI) in natural waters, Anal. Bioanal. Chim. 375 (2003) 698–702.
[15] S. Sadeghi, A. Akbarzadeh Mofrad, Synthesis of a new ion imprinted polymer material for separation and preconcentration of traces of uranyl ions, React. Funct. Polym. 67 (2007) 966–976.
[16] S. Sadeghi, E. Shykhzadeh, Solid phase extraction using silica gel functionalized with sulfasalazine for preconcentration of uranium (VI) ions from water samples, Microchim. Acta 163 (2008) 313–320.
[17] S. Sadeghi, E. Shykhzadeh, Solid phase extraction using silica gel modified with murexide for preconcentration of uranium (VI) ions from water samples, J. Hazard. Mater. 163 (2009) 861–869.
[18] A. Henglein, Small-particle research: physicochemical properties of extremely small colloidal metal and semiconductor particles, Chem. Rev. 89 (1989) 1861–1873.
[19] A.F. Ngomsik, A. Bee, M. Draye, G. Cote, V. Cabuil, Magnetic nano- and microparticles for metal removal and environmental applications: a review, C.R. Chimie 8 (2005) 963–970.
[20] M. Faraji, Y. Yamini, A. Saleh, M. Rezaee, M. Ghambarian, R. Hassani, A nanoparticle-based solid-phase extraction procedure followed by flow injection inductively coupled plasma-optical emission spectrometry to determine some heavy metal ions in water samples, Anal. Chim. Acta 659 (2010) 172–177.
[21] W. Yantasee, C.L. Warner, T. Sangvanich, R.S. Addleman, T.G. Carter, R.J. Wiacek, G.E. Fryxell, C. Timchalk, M.G. Warner, Removal of heavy metals from aqueous

systems with thiol functionalized superparamagnetic nanoparticles, Environ. Sci. Technol. 41 (2007) 5114–5119.
[22] J.S. Suleiman, B. Hu, H. Peng, C. Huang, Separation/preconcentration of trace amounts of Cr, Cu and Pb in environmental samples by magnetic solid-phase extraction with Bismuthiol-II-immobilized magnetic nanoparticles and their determination by ICP-OES, Talanta 77 (2009) 1579–1583.
[23] S.-H. Huang, D.-H. Chen, Rapid removal of heavy metal cations and anions from aqueous solutions by an amino-functionalized magnetic nano-adsorbent, J. Hazard. Mater. 163 (2009) 174–179.
[24] J.H. Jang, H.B. Lim, Characterization and analytical application of surface modified magnetic nanoparticles, Microchim. J. 94 (2010) 148–158.
[25] M. Ghaedi, B. Karami, F. Sh Ehsani, M. Marahel, Soylak, preconcentration–separation of Co^{2+}, Ni^{2+}, Cu^{2+} and Cd^{2+} in real samples by solid phase extraction of calyx[4] resorcinarene modified Amberlite XAD-16 resin, J. Hazard. Mater. 172 (2009) 802–808.
[26] X. Song, J. Li, J. Wang, L. Chen, Quercetin molecularly imprinted polymers: preparation, recognition and properties as sorbent for solid phase extraction, Talanta 80 (2009) 694–702.
[27] A. Torreggiani, M. Tamba, A. Trinchero, S. Bonora, Copper(II)–quercetin complexes in aqueous solutions: spectroscopic and kinetic properties, J. Mol. Struct. 744–747 (2005) 759–766.
[28] R. Gheshlaghi, J.M. Scharer, M. Moo-Young, P.L. Douglas, Application of statistical design for the optimization of amino acid separation by reverse-phase HPLC, Anal. Biochem. 383 (2008) 93–102.
[29] S.J. Kalil, F. Maugeri, M.I. Rodrigues, Response surface analysis and simulation as a tool for bioprocess design and optimization, Process Biochem. 35 (2000) 539–550.
[30] P. Berger, N. Adelman, K.J. Beckman, D.J. Campbell, A.B. Ellis, G.C. Lisensky, Preparation, and properties of an aqueous ferrofluid, J. Chem. Educ. 76 (1999) 943–948.
[31] W. Stöber, A. Fink, E. Bohn, Controlled growth of monodisperse silica spheres in the micron size range, J. Colloid Interface Sci. 26 (1968) 62–69.
[32] G.E.P. Box, K.B. Wilson, J. Roy, On the experimental attainment of optimum conditions, Stat. Soc. Ser. B 13 (1951) 1–45.
[33] H. Arabi, S. Nateghi, S. Sadeghi, Synthesis and effect of some parameters through reverse micelles route of iron oxide nanoparticles, Solid State Phenomen. 152-153 (2009) 205–208.
[34] H.P. Klug, L.E. Alexander, X-ray Diffraction Procedures for Polycrystalline and Amorphous Materials, John Wiley & Sons, New York, 1962, p. 491.
[35] K. Nakamoto, Infrared Spectra of Inorganic and Coordination Compounds, 2nd ed., Wiley, London, UK, 1970.
[36] V.S. Zaitsev, D.S. Filimonov, I.A. Presnyakov, R.J. Gambino, B. Chu, Physical and chemical properties of magnetite and magnetite-polymer nanoparticles and their colloidal dispersions, J. Colloid Interface Sci. 212 (1999) 49–57.
[37] M. Khani, Statistical analysis and isotherm study of uranium biosorption by *Padina* sp. Algae biomass, Environ. Sci. Pollut. Res. 18 (2011) 790–799.
[38] H. Fabre, Robustness testing in liquid chromatography and capillary electrophoresis, J. Pharm. Biomed. Anal. 14 (1996) 1125–1132.
[39] H. Sereshti, V. Khojeh, S. Samadi, Optimization of dispersive liquid–liquid microextraction coupled with inductively plasma-optical emission spectrometry with the aid of experimental design for simultaneous determination of heavy metals in natural waters, Talanta 83 (2011) 885–890.
[40] I.J. Langmuir, The adsorption of gases on plane surfaces of glass, mica and platinum, J. Am. Chem. Soc. 40 (1918) 1361–1403.
[41] Y. Jung, S. Kim, S.-J. Park, J.M. Kim, Application of polymer-modified nanoporous silica to adsorbents of uranyl ions, Colloid. Surf. A 313–314 (2008) 162–166.
[42] T. Caykara, S.S. Alaslan, R. Inam, Competitive adsorption of uranyl ions in the presence of Pb(II) and Cd(II) ions by poly(glycidyl methacrylate) microbeads carrying amidoxime groups and polarographic determination, J. Appl. Polymer Sci. 104 (2007) 4168–4172.
[43] I.M. Ismail, M. Nogami, K. Suzuki, Effect of pore diameter of TMMA chelating resin beads on the adsorption properties of U(VI) and Ce(III) from different media, Sep. Purif. Technol. 31 (2003) 231–239.
[44] X. Shuibo, Z. Chun, Z. Xinghuo, Y. Jing, Z. Xiaojian, W. Jingsong, Removal of uranium (VI) from aqueous solution by adsorption of hematite, J. Environ. Radioact. 100 (2009) 162–166.
[45] B. Cyriac, B.K. Balaji, A novel method of synthesizing solid phase adsorbent silica modified with xylenol orange: application for separation, pre-concentration and determination of uranium in calcium rich hydro-geochemical samples and sea water-Part 1, Microchim. Acta 171 (2010) 33–40.
[46] S. Yusan, N. Yenil, S. Kuzu, M.A.A. Aslani, Properties of Uranium(VI) adsorption by methyl 3-O-acetyl-5,6-dideoxy-(S)-1,2-trichloroethylidene-r-D-xylo-hept-5(E)-eno-1,4-furano-uronate, J. Chem. Eng. Data 56 (2011) 2013–2019.